

6-2018


Femoral Neck Stress in Older Adults During Stair Ascent and Descent

Chen Deng
Iowa State University

Jason C. Gillette
Iowa State University, gillette@iastate.edu

Timothy R. Derrick
Iowa State University, tderrick@iastate.edu

Follow this and additional works at: https://lib.dr.iastate.edu/kin_pubs

 Part of the [Exercise Science Commons](#), [Motor Control Commons](#), [Movement and Mind-Body Therapies Commons](#), [Musculoskeletal, Neural, and Ocular Physiology Commons](#), and the [Psychology of Movement Commons](#)

The complete bibliographic information for this item can be found at https://lib.dr.iastate.edu/kin_pubs/52. For information on how to cite this item, please visit <http://lib.dr.iastate.edu/howtocite.html>.

This Article is brought to you for free and open access by the Kinesiology at Iowa State University Digital Repository. It has been accepted for inclusion in Kinesiology Publications by an authorized administrator of Iowa State University Digital Repository. For more information, please contact digirep@iastate.edu.

Femoral Neck Stress in Older Adults During Stair Ascent and Descent

Abstract

A detailed understanding of the hip loading environment is needed to help prevent hip fractures, minimize hip pain, rehabilitate hip injuries, and design osteogenic exercises for the hip. The purpose of this study was to compare femoral neck stress during stair ascent and descent and to identify the contribution of muscles and reaction forces to the stress environment in mature adult subjects ($n = 17$; age: 50–65 y). Motion analysis and inverse dynamics were combined with musculoskeletal modeling and optimization, then used as input to an elliptical femoral neck cross-sectional model to estimate femoral neck stress. Peak stress values at the 2 peaks of the bimodal stress curves (stress vs time plot) were compared between stair ascent and descent. Stair ascent had greater compressive stress than descent during the first peak at the anterior (ascent: $-18.0 [7.9]$ MPa, descent: $-12.9 [5.4]$ MPa, $P < .001$) and posterior (ascent: $-34.4 [10.9]$ MPa, descent: $-27.8 [10.1]$ MPa, $P < .001$) aspects of the femoral neck cross section. Stair descent had greater tensile stress during both peaks at the superior aspect (ascent: $1.3 [7.0]$ MPa, descent: $24.8 [9.7]$ MPa, peak 1: $P < .001$; ascent: $15.7 [6.1]$ MPa, descent: $18.0 [8.4]$ MPa, peak 2: $P = .03$) and greater compressive stress during the second peak at the inferior aspect (ascent: $-43.8 [9.7]$ MPa, descent: $-51.1 [14.3]$ MPa, $P = .004$). Understanding this information can provide a more comprehensive view of bone loading at the femoral neck for older population.

Keywords

bone stresses, hip contact force, estimated muscle force

Disciplines

Exercise Science | Kinesiology | Motor Control | Movement and Mind-Body Therapies | Musculoskeletal, Neural, and Ocular Physiology | Psychology of Movement

Comments

This accepted article is published as Deng C, Gillette JC, & Derrick TR. (2018). Femoral neck stress in older adults during stair ascent and descent. *Journal of Applied Biomechanics*, 34(3);191-198. <https://doi.org/10.1123/jab.2017-0122>. Posted with permission.

1 **Title:** FEMORAL NECK STRESS IN OLDER ADULTS DURING STAIR ASCENT AND
2 DESCENT

3 Manuscript ID JAB.2017-0122.R1

4 **Authors:** Chen Deng, Jason C. Gillette, Timothy R. Derrick

5 Iowa State University, Ames, IA, USA

6 **Correspondence address:**

7 Chen Deng, M.S.

8 Department of Kinesiology, Iowa State University

9 Forker 105, Ames, IA, 50011

10 Email: chend@iastate.edu;

11 **Paper Type:** original research article

12 **Conflict of interest:** none.

ABSTRACT

13
14
15
16
17
18
19
20
21
22
23
24
25
26
27
28
29
30
31
32
33

A detailed understanding of the hip loading environment is needed to help prevent hip fractures, minimize hip pain, rehabilitate hip injuries and design osteogenic exercises for the hip. The purpose of this study was to compare femoral neck stress during stair ascent and descent and to identify the contribution of muscles and reaction forces to the stress environment in mature adult subjects (n=17; age: 50-65 years). Motion analysis and inverse dynamics were combined with musculoskeletal modelling and optimization, then used as input to an elliptical femoral neck cross-section model to estimate femoral neck stress. Peak stress values at the two peaks of the bimodal stress curves (stress vs. time plot) were compared between stair ascent and descent. Stair ascent had greater compressive stress than descent during the first peak at the anterior (ascent: -18.0 ± 7.9 MPa, descent: -12.9 ± 5.4 MPa, $p < 0.001$) and posterior (ascent: -34.4 ± 10.9 MPa, descent: -27.8 ± 10.1 MPa, $p < 0.001$) aspects of the femoral neck cross section. Stair descent had greater tensile stress during both peaks at the superior aspect (ascent: 1.3 ± 7.0 MPa, descent: 24.8 ± 9.7 MPa, peak 1: $p < 0.001$; ascent: 15.7 ± 6.1 MPa, descent: 18.0 ± 8.4 MPa, peak 2: $p = 0.028$) and greater compressive stress during the second peak at the inferior aspect (ascent: -43.8 ± 9.7 MPa, descent: -51.1 ± 14.3 MPa, $p = 0.004$). Understanding this information can provide a more comprehensive view of bone loading at the femoral neck for older population.

Key words: Femoral neck, bone stresses, stair ascent and descent, hip moments, estimated muscle force

Word Count: 4145

34

Introduction

35 Femoral neck fracture is a serious injury that can play an important role in morbidity and
36 mortality among individuals, especially older adults ¹. With the overall mortality rate of hip
37 fractures at 14.0-21.6%, the estimated 290,000 cases expected by 2030 this injury will result in a
38 growing health problem for an aging population ²⁻⁴. If structural failure is of concern, external
39 loading, internal loading, bone geometry and bone material properties are the main factors that
40 need to be investigated ⁵. Therefore, it is important to investigate the loading environment of the
41 femoral neck during activities of daily living such as stair negotiation. Modification of these
42 activities may minimize further damage to an injured site, while still encouraging osteogenesis as
43 a preventative measure.

44 A detailed analysis of the proximal femur load is necessary to understand mechanisms of
45 failure. The femoral neck positions the hip abductor muscles away from the joint center so that
46 adequate abductor torque can be generated to counter the large adductor torque caused by weight
47 of the torso. In general, the torso weight vector acting on the femoral neck causes bending stress
48 that results in inferior surface compression and superior surface tension during the single support
49 phase of gait. Axial stress, caused by a component of the torso weight and the muscles that cross
50 the hip, acts in compression evenly throughout the cross section and sums with the bending
51 stress. This tends to increase the compression on the inferior surface and decrease the tension on
52 the superior surface. The probability of bone failure may be altered through changes to the
53 magnitude or frequency of loading (fatigue fractures) ⁶, insufficient bone strength (fragility
54 fractures) ⁷, or a combination of these factors.

55 Several studies have examined the joint loading environment of the proximal femur
56 during stair ascent and descent ⁸⁻¹², yet there is still uncertainty concerning which activity
57 produces greater loads. This lack of clarity is partly due to the difficulty in measuring the
58 variables that are directly responsible for damage. The most direct measures of hip loading are
59 from instrumented prostheses ⁸. These devices transmit the hip joint forces via a wireless signal
60 to a computer while patients perform various activities. It should be noted that these
61 measurements were performed on a small number of subjects (n = 2-4) and the subjects were
62 atypical since they had undergone hip replacement surgery within 11-31 months prior to testing.
63 Although this procedure provides a direct measure of the hip joint forces, the invasive nature and
64 limited subject pool reduces the practicality of this protocol in most laboratory and clinic
65 settings.

66 Several studies have utilized inverse dynamics and rigid body models to estimate net
67 joint moments and reaction forces during stair ascent and descent ^{13, 14}. As an estimate of femoral
68 neck loading these measures give only a rough approximation. Both the net joint moment and the
69 reaction force neglect the effects of co-contracting muscles and fail to consider the size of the
70 bone in determining the potential for failure.

71 Using procedures developed for mechanics of materials, stress analysis is an alternative
72 method of estimating bone loads. Inverse dynamics are combined with musculoskeletal
73 modelling and estimated muscle forces ¹⁵ to quantify hip contact forces and ultimately stresses or
74 strains in the bone ¹⁶. Forces, moments and bone structure are all taken into account so that
75 excessive loading can be determined from any source. The purpose of this study was to compare
76 hip joint contact forces and stress on a cross section of the femoral neck during stair ascent and
77 descent. In this study, a detailed analysis of these stresses was performed by decomposing the

78 sources of the stress into those due to muscle forces, muscle moments, reaction forces and
79 reaction moments. It was hypothesized that increased hip extensor muscle forces required to
80 generate greater hip extensor moments during stair ascent^{13, 14} would cause femoral neck
81 compression stresses to be greater than during stair descent.

82 **Methods**

83 Seven male (age: 60 ± 6 yr; body mass: 75 ± 14 kg; height: 1.73 ± 0.05 m) and ten female
84 subjects (age: 57 ± 5 yr; body mass: 67 ± 8 kg; height: 1.67 ± 0.05 m) who were free from lower
85 limb injuries volunteered to participate. Before participation, they signed a written informed
86 consent that had been approved by the Iowa State University Human Subjects Review Board.

87 Body mass, height, and right lower extremity segment lengths, widths, and
88 circumferences were measured. Eighteen reflective markers were placed on anatomical
89 landmarks of the trunk, pelvis, and right lower extremity with a minimum of 3 markers/segment:
90 toe, heel for the foot segment; anterior/posterior leg for the leg segment; anterior thigh, right hip
91 for the thigh segment; left hip, right/left ASIS and sacrum for the pelvis segment; medial/lateral
92 ankle can be considered both in the foot and leg segments, medial/lateral knee can be considered
93 both in the leg and thigh segments. All anthropometric measurements and marker placements
94 were performed by the same researcher. A static trial was collected with the subject in
95 anatomical position to estimate joint center locations by the markers on the joints and then
96 medial side markers of the lower extremity were removed. All subjects performed five trials of
97 stair ascent and five trials of descent (three-step staircase, height of each stair: 19 cm) at their
98 normal comfortable speed. The left foot started each trial, and the right foot contacted the force
99 platform on the second step. AMTI force platforms (1600 Hz, AMTI, Watertown, MA) were

100 placed on the two lower stairs to measure ground reaction forces. Motion data were collected
101 using an 8-camera system (160 Hz, Vicon MX, Centennial, CO).

102 Ground reaction forces and motion data were filtered using a fourth-order, low-pass
103 Butterworth filter with a cutoff frequency of 6 Hz^{17,18}. The stance phase cycle for stair
104 ascent/descent began when the right foot contacted the force platform and finished with toe-off.
105 All gait cycles were normalized into a percentage of the stance phase. A rigid body model was
106 used with inverse dynamics procedures to estimate three-dimensional joint moments and reaction
107 forces at the ankle, knee, and hip. Segment masses, center of mass locations, and moments of
108 inertia were obtained by the equations of Vaughan et al.¹⁹.

109 An individually scaled musculoskeletal model based on the joint and muscle definitions
110 of Arnold et al.²⁰ was implemented in Matlab to estimate the dynamic muscle-tendon length and
111 velocity adjusted maximal muscle forces, muscle moment arms and orientations for 44 lower
112 limb muscles using the three dimensional segment angles obtained during the trials. Static
113 optimization was used to select a set of muscle forces that minimized the sum of the squared
114 muscle stresses²¹ and balanced using the sagittal plane hip, knee and ankle moments, frontal
115 plane hip moment and the transverse plane hip and ankle moments. Solutions were also
116 constrained by the maximal dynamic muscle forces estimated with the musculoskeletal model.

117
$$\text{Min } \sum_{i=1}^{44} (F_i/A_i)^2 \quad \text{Subject to: } r_{ij} \times F_i = M_j \quad 0 \leq F_i \leq \text{Max dynamic } F_i$$

118 For the *i*th muscle: F_i is estimated muscle force, A_i is the cross-sectional area, r_{ij} is the
119 moment arm for the *j*th joint moment, and M_j is the *j*th joint moment.

120 Hip joint reaction forces were summed with muscle forces crossing the hip joint to
121 obtain hip contact forces that were then transformed into the thigh coordinate system. The thigh

122 coordinate system has the long axis of femur as longitudinal direction (y-axis), the cross product
123 of y-axis and the vector from knee joint center to lateral knee marker as the anterior-posterior
124 axis (x-axis), the cross product of x- and y-axis as medial-lateral axis (z-axis). Forces and
125 moments acting at the centroid of the femoral neck cross section were calculated by transforming
126 the hip contact forces into a femoral neck coordinate system and using the techniques and
127 assumptions of beam theory. The femoral neck coordinate system had one axis (z-axis) parallel
128 to the longitudinal axis of the neck and one orthogonal axis pointing approximately forward (x-
129 axis) and the third (y-axis) obtained by the cross product of the first two.

130 An elliptical bone model (Figure 1) was used to estimate stresses on the superior, inferior,
131 anterior and posterior surface of the femoral neck. Age and gender specific subperiosteal width
132 and cortical width ²² were used to create quadratic prediction equations for the outer and inner
133 diameters along the superior/inferior axis.

134 Male Outer Diameter = $-0.0004 \times \text{age}^2 + 0.0962 \times \text{age} + 32.042$, $R^2 = 0.982$

135 Male Inner Diameter = $-0.0004 \times \text{age}^2 + 0.1152 \times \text{age} + 27.476$, $R^2 = 0.987$

136 Female Outer Diameter = $-0.0004 \times \text{age}^2 + 0.1036 \times \text{age} + 26.662$, $R^2 = 0.99$

137 Female Inner Diameter = $-0.0003 \times \text{age}^2 + 0.1102 \times \text{age} + 22.445$, $R^2 = 0.994$

138 Where age is in years and diameters are in millimeters.

139 Anterior/posterior diameters were estimated by multiplying the superior/inferior diameters by the
140 ratio of maximal to minimal diameters (male: 1.16 ± 0.04 ; female 1.26 ± 0.03) ²³.

141 The stress estimation formulas were as follows:

142 $\sigma_{\text{superior}} = \sigma(-M_{\text{ap}}) + \sigma(F_{\text{axial}})$ $\sigma_{\text{inferior}} = \sigma(M_{\text{ap}}) + \sigma(F_{\text{axial}})$

143 $\sigma_{\text{anterior}} = \sigma(M_{\text{ml}}) + \sigma(F_{\text{axial}})$ $\sigma_{\text{posterior}} = \sigma(-M_{\text{ml}}) + \sigma(F_{\text{axial}})$

144 Where σ_{superior} is the stress on the superior aspect of the femoral neck, σ_{inferior} is the
145 stress on the inferior aspect, σ_{anterior} is the stress on the anterior aspect, $\sigma_{\text{posterior}}$ is the stress on
146 the posterior aspect, $\sigma(M_{\text{ml}})$ is the stress generated by sagittal plane moment, $\sigma(M_{\text{ap}})$ is the
147 stress generated by frontal plane moment and $\sigma(F_{\text{axial}})$ is the stress caused by the axial force.
148 Negative values indicate compressive stress and positive values indicate tensile stress.

149 The total stress on the femoral neck cross section is caused by a combination of the joint
150 reaction force and the muscle forces. An analysis was undertaken to investigate how these
151 variables independently affect the stress environment. The joint reaction force and muscle forces
152 have the potential to compress the elliptical cross section of the femoral neck and to produce
153 bending about the major and minor axes. The stress analysis was performed using each of these
154 four components separately: 1) the joint reaction force compression component, 2) the muscle
155 force compression component, 3) the joint reaction force bending/moment component, and 4) the
156 muscle bending/moment component. The total muscle component was the sum of 2 and 4, the
157 total reaction component was the sum of 1 and 3, and the total stress was the sum of 1-4.

158 Previous validation work explored the correlations between elliptical bone model and CT
159 bone model for the tibia bone, which showed that the correlation of peak tensile stress on the
160 anterior site was 0.89, and the peak compressive stress on the posterior site was 0.96²⁴. These
161 correlations were considered to be sufficiently high to perform a repeated measures statistical
162 analysis. Since the shape of the femoral neck cross section is a closer fit to the elliptical model
163 than the tibia, it is reasonable to assume that the correlations of stresses on the femoral neck
164 between the elliptical model and a CT model should be even higher than the outcomes from the
165 tibia study²⁴. Moreover, this elliptical model was selected since it provided a method to

166 determine stress curves for the entire stance phase and allows for the breakdown of individual
167 stress components in a more computationally efficient manner than with a finite element model.

168 The primary dependent variable was stress, but peak longitudinal, medial-lateral and
169 anterior-posterior hip contact forces were also calculated to help explain results. Pairwise t-tests
170 were used to compare the peak hip joint contact forces between stair ascent and descent. For the
171 stress analysis, the independent variables were the direction of travel (ascent vs descent) and the
172 site or location of the stress on the femoral neck cross section (anterior, posterior, superior and
173 inferior). The stress was estimated at the two time points during the stance phase that
174 corresponded with the two peak values on the stress by time curves. The stress on the superior
175 aspect of the cross section did not have a consistent first peak during stair ascent so the average
176 time of the peak during descent was used. In order to get a more holistic view of the relationship
177 between these variables, the stress was decomposed into four sources (muscle force, muscle
178 moment, reaction force and reaction moment). The average of 5 trials for each direction was
179 used for statistical analysis. Positive stress values indicate a tensile stress and negative values
180 indicate a compressive stress throughout this paper, however statistics were performed on the
181 absolute value of the stress, making tensile and compressive stress clinically equivalent. A two-
182 way repeated-measures MANOVA was used to compare the differences between the four sites
183 on the femoral neck and the direction as well as a site by direction interaction (SPSS, IBM
184 Corp). Univariate ANOVAs were performed given a significant multivariate statistic. Pairwise t-
185 tests were used to compare the stresses at the same site between stair ascent and descent. If
186 sphericity was violated a Greenhouse-Geisser correction was performed. Force and moment
187 contributions to the stress were not statistically compared but used to explain stress magnitudes.
188 The alpha level was set at .05 for all statistical tests.

189

Results

190 Hip joint contact forces acts at the center of the femoral head (hip joint center) and are
191 presented in the thigh coordinate system (Figure 2). The anterior-posterior and longitudinal forces
192 tended to be bimodal with the first peak occurring at approximately 20% of stance and the second
193 peak occurring at approximately 80% of stance. In general, the peak 1 forces were greater than
194 peak 2. The laterally directed component often had only a single peak value occurring at 20% of
195 stance. This component of the hip joint contact force was statistically greater during ascent (ascent:
196 2.51 ± 0.39 BW, descent: 1.37 ± 0.24 BW, $p < 0.001$). The peak 1 posteriorly directed component
197 of the hip joint contact force was also greater in ascent (ascent: 1.44 ± 0.29 BW, descent: $0.85 \pm$
198 0.19 BW, $p < 0.001$) while the peak 2 force was greater during descent (ascent: 0.51 ± 0.14 BW,
199 descent: 0.72 ± 0.20 BW, $p = 0.002$). Peak hip contact forces in the longitudinal direction had the
200 greatest magnitudes and were directed distally. They had the same trend as the posteriorly directed
201 force peaks – peak 1 was greater during ascent (ascent: 4.57 ± 0.53 BW, descent: 3.95 ± 0.49 BW,
202 $p = 0.001$) while peak 2 was greater during descent (ascent: 3.16 ± 0.38 BW, descent: 3.77 ± 0.63
203 BW, $p = 0.006$).

204 MANOVA results revealed a significant interaction between direction (ascent vs descent)
205 and site (anterior, posterior, superior and inferior) in peak stress ($p < 0.001$) indicating a
206 significant interaction in at least one of the peak values. MANOVA main effects were also
207 significant for direction ($p = 0.017$), and site ($p < 0.001$).

208 Univariate results indicated that the direction by site interaction was present for both peak
209 1 ($p < 0.001$) and peak 2 ($p = 0.013$) stresses. Figure 3 and 4 illustrate these interactions by
210 showing changes in the peak stress values between stair ascent and descent for each site. The
211 interaction during peak 1 was due to increases in stair descent stresses on the superior and

212 inferior aspects of the femoral neck but decreases in stair descent stresses on the anterior and
213 posterior aspects. The interaction during peak 2 was due to a greater increase in stair descent
214 stress on the inferior aspect of the femoral neck relative to the other three sites. Main effect
215 statistics are not presented due to the significant interactions. Post-hoc paired t-tests were used to
216 compare ascent vs descent total stress values at each site and peak (Table 1 and 2).

217 During both stress peaks the dominant loading in the femoral neck was compressive and
218 occurred on the inferior region of the femoral neck during both ascent and descent. Compressive
219 stress at the inferior site was greater during stair descent than ascent for the second stress peak (-
220 43.8 ± 9.7 MPa (peak 2-Ascent-Inferior), -51.1 ± 14.3 MPa (peak 2-Descent-Inferior), $p = 0.004$).

221 Peak tensile stresses occurred in the superior region and were greater during stair descent
222 during both peaks (1.3 ± 7.0 MPa (peak 1-Ascent-Superior), 24.8 ± 9.7 MPa (peak 1-Descent-
223 Superior), $p < 0.001$; and 15.7 ± 6.1 MPa (peak 2-Ascent-Superior), 18.0 ± 8.4 MPa (peak 2-
224 Descent-Superior), $p = 0.028$) compared to stair ascent.

225 The anterior and posterior regions were generally in compression. Peak compressive
226 stress on the anterior aspect of the femoral neck was greater during stair ascent (-18.0 ± 7.9 MPa
227 (peak 1-Ascent-Anterior)) compared to descent (-12.9 ± 5.4 MPa (peak 1-Descent-Anterior)) at
228 peak 1 ($p < 0.001$). Likewise, the posterior aspect had an increased compressive stress for stair
229 ascent (-34.4 ± 10.9 MPa (peak 1-Ascent-Posterior)) than descent (-27.8 ± 10.1 MPa (peak 1-
230 Descent-Posterior)) at peak 1 ($p < 0.001$).

231 Based on the estimations from the model, the stress caused by the reaction component
232 was calculated separately from the stress caused by the muscle component so that distinct
233 contributions to the stress load could be assessed (Table 1). Overall, the greatest stresses were
234 compressive with the reaction component causing greater stress magnitudes than the muscle

235 component. The three greatest stress magnitudes caused by the reaction component were $-86.6 \pm$
236 17.1 MPa (peak 1-Ascent-Inferior), -80.6 ± 26.2 MPa (peak 1-Descent-Inferior), and $-73.0 \pm$
237 19.1 MPa (peak 2-Ascent-Inferior) while the three greatest stress magnitudes caused by the
238 muscle component were -63.1 ± 18.5 MPa (peak 1-Ascent-Superior), -48.7 ± 17.3 MPa (peak 1-
239 Descent-Posterior), and -43.8 ± 17.8 MPa (peak 2-Ascent-Superior).

240 Stresses were also decomposed according to the contributions from moments and forces.
241 In general the contribution to the peak stress was dominated by the moments. The greatest
242 compressive stress was at the inferior site during peak 1 of stair descent, the reaction force
243 produced -4.1 ± 0.9 MPa of compression and the muscle forces produced -13.0 ± 3.0 MPa.
244 However, the reaction moment produced 36.4 ± 18.1 MPa of tensile stress and the muscle
245 moment produced -76.6 ± 25.8 MPa of compressive stress.

246 Discussion

247 The hypothesis that hip contact forces would be significantly greater during stair ascent
248 was not universally supported by the results. Peak hip contact forces were greater during stair
249 ascent than descent at peak 1, but at peak 2 the posteriorly and distally directed hip contact forces
250 were greater during stair descent than ascent (Figure 2). These shapes of the contact force curves
251 were mirrored by the muscle activity in the hip extensor muscles during ascent and descent
252 (Figures 6 and 7).

253 The hypothesis that femoral neck stress would be significantly greater during stair ascent
254 was also not supported by the results. We estimated femoral neck stresses at four sites on the
255 femoral neck during stair ascent and descent for older adults and then analyzed the sources of
256 stress. The MANOVA main effect of ascent/descent on femoral neck stresses ($p = 0.017$) and the
257 interaction effect between directions and femoral neck sites ($p < 0.001$) were both significant.

258 The univariate interaction effects for both stress peak 1 ($p < 0.001$) and peak 2 ($p = 0.013$) were
259 significant. Results indicates that 1) at some sites the stresses were greater during ascent than
260 descent, in other sites the stresses were greater during descent compared to ascent (Figure 3); 2)
261 stress change patterns were similar among different sites, but the change of slope between stair
262 ascent and descent for some sites were much greater than other sites (Figure 4). Both peak tensile
263 stress at the superior site (both peaks) and peak compressive stress at the inferior site (peak 2)
264 showed greater stress during stair descent. The peak 1 stress during early stair descent could be a
265 consequence of a relatively extended position of the hip and knee during this phase of the decent.
266 This erect posture may allow the ground reaction force vector to be directed through the joints
267 and minimize the ability of the muscles to absorb the energy of the downward moving mass.
268 This can be seen in the EMG activity of the hip extensor muscles during stair ascent and descent
269 ²⁵.

270 An examination of the stress caused by the reaction force/moment compared to the
271 muscle force/moment highlights how this relationship affects the total stress environment. In
272 general, any time the reaction force/moment caused a stress greater than 25 MPa (compressive or
273 tensile) the muscles contracted to produce bending in the opposite direction and thus reduced the
274 total stress. For example, the weight and acceleration of the torso caused a reaction force to push
275 down on the head of the femur during P1 ascent. This bent the neck concave inferior and caused
276 64.4 ± 17.1 MPa of tensile stress on the superior aspect of the neck. However, hip abductor and
277 extensor muscles were activated at that time and they produce concave superior bending. This
278 compressed the superior region with a stress of -63.1 ± 18.5 MPa. The net result was minimal
279 stress (1.3 ± 7.0 MPa) because the tensile stress cancelled the compressive stress in this region.
280 During descent the reaction component caused 67.5 ± 24.7 MPa of tensile stress while the

281 muscle component was reduced to -42.7 ± 19.0 MPa of compression. This resulted in increased
282 tension on the superior surface (24.8 ± 9.7 MPa) compared to ascent (1.3 ± 7.0 MPa).

283 On both superior and inferior surfaces of femoral neck, the muscle component produced
284 stresses opposite to, but smaller in magnitude than the stresses produced by the reaction
285 force/moment, so greater stresses from muscle can be an effective way to minimize the net
286 stresses on these 2 surfaces of femoral neck. Stair descent tended to decrease the stresses
287 produced by muscle compared to stair ascent. This suggests that the ability of the muscles to
288 reduce bone stress may be minimized during stair descent.

289 The stress produced by forces is predominantly compressive, while stress produced by
290 moments creates compression on the inside of the curvature and tension on the outside portion.
291 In general, the magnitude of the stress caused by moments was greater than the magnitude
292 caused by forces at most sites and directions. The stress caused by the moment dominated on
293 both the inferior and superior regions but the contribution of the moments was generally reduced
294 at the anterior and posterior sites.

295 There are several limitations associated with these procedures. An ellipse model of the
296 femoral neck cross-section was created for each subject based on age and gender. Derrick et al.²⁴
297 showed that a homogeneous elliptical model such as this could be favorably compared to a more
298 detailed nonhomogeneous model derived from a CT scan of the tibial cross-section (r-squared =
299 0.89 for the peak tensile stress on the anterior site, and 0.96 for the peak compressive stress on
300 the posterior site). Moreover, the shape of femoral neck cross section is more elliptical than the
301 cross section of the tibia, suggesting these correlations are conservative when compared to the
302 current study. Muscles were scaled to the individual but modeled with standardized insertions,
303 origins and contraction properties and the muscle forces were estimated using static optimization

304 with a cost function that minimized muscle stresses. Individual differences in the muscle
305 properties or non-optimal sequencing of muscle activity could influence the muscle forces.

306 Muscle optimization does not guarantee an exact replication of the muscle force patterns.
307 The process assumes that the activation of muscles follows the rules of the cost function
308 (minimization of the sum of the muscle stress squared). Differences between the estimated and
309 actual muscle force may occur if a person uses an alternate pattern of recruitment. Estimated hip
310 extensor muscle forces were compared to EMG data ²⁵ in the literature to assess the accuracy of
311 this estimation. Figures 6 and 7 show the comparison between hip extensor muscle forces and
312 EMG activity (including biceps femoris long head, semimembranosus, upper gluteus maximus,
313 and gluteus medius muscle forces). The cross-correlation between the two EMG and muscle
314 force shows acceptable agreement for stair ascent (0.725) but a lower cross-correlation value
315 (0.162) for descent. This lower cross-correlation during descent was due to the peaks of EMG
316 curves being shifted closer to contact and toe-off.

317 The lower limb joint center (ankle/knee/hip) calculations were based on the reflective
318 markers placed on the bony landmarks of each joint. Inaccuracies in marker placement may
319 result in errors in the estimation of joint center locations. These inaccuracies may decrease the
320 accuracy of joint moment estimation based on the inverse dynamics method ²⁶. Although the
321 repeated measures nature of this study likely reduces the effect of inaccurate marker placement it
322 does not insure that the errors in marker placement or marker movement are the same between
323 ascent and descent.

324 In this study, contact force and femoral neck stress were analyzed to evaluate loading at
325 the hip joint during stair ascent and descent for older population. Joint contact forces give a good
326 estimate of the loading between the femoral head and the pelvic acetabulum. Bone stresses are

327 more directly related to the loads that cause the bone to fracture and include the influence of
328 muscle forces, reaction forces and bone geometry. We found that the greatest hip contact forces
329 occurred at about 20% of stance while ascending the stairs. Stresses in the femoral neck were
330 generally, but not universally, greater during stair descent. Stress variations on the periphery of
331 the femoral neck cross-section were large with the inferior region receiving the greatest stress
332 values. Combining contact forces and bone stresses could help future studies analyze loading
333 conditions in a more comprehensive way for other physical activities.

334

335
336
337
338
339
340
341
342
343
344
345
346
347
348
349
350
351
352
353
354
355
356

References

1. Graves EJ. Detailed diagnoses and procedures, national hospital discharge survey. *Vital and Health Statistics*. 1990; 13(113):1-225.
2. Kenzora J, McCarthy R, Drennan L, Sledge, C. Hip Fracture Mortality: Relation to age, treatment, preoperative illness, time of surgery, and complications. *Clinical Orthopaedics & Related Research*. Section I: symposium: reconstructive hip and knee surgery. *Clin Orthop Relat R*. 1984.
3. White BL, Fisher WD, Laurin CA. Rate of mortality for elderly patients after fracture of the hip in the 1980's. *J Bone Joint Surg*. 1990; 69: 1335-1340.
4. Stevens JA, Rudd RA. The impact of decreasing U.S. hip fracture rates on future hip fracture estimates. *Osteoporosis Int*. 2013; 24(10): 2725-2728.
5. Lotz JC, Cheal EJ, Hayes WC. Stress distributions within the proximal femur during gait and falls: Implications for osteoporotic fracture. *Osteoporosis Int*. 1995; 5: 252.
6. Zadpoor AA, Nikooyan AA. The relationship between lower-extremity stress fractures and the ground reaction force: A systematic review. *Clin Biomech*. 2011; 26(1): 23-28.
7. Greenspan SL, Myers ER, Maitland LA, Resnick NM, Hayes WC. Fall Severity and Bone Mineral Density as Risk Factors for Hip Fracture in Ambulatory Elderly. *JAMA*. 1994; 271(2):128-133.
8. Bergmann G, Graichen F, Siraky J, Jendrzynski H, Rohlmann A. Multichannel strain gauge telemetry for orthopaedic implants. *J Biomech*. 1988; 21: 169-176.
9. Bergmann G, Graichen F, Rohlmann A. Hip joint forces during walking and running, measured in two patients. *J Biomech*. 1993; 26: 969-990.

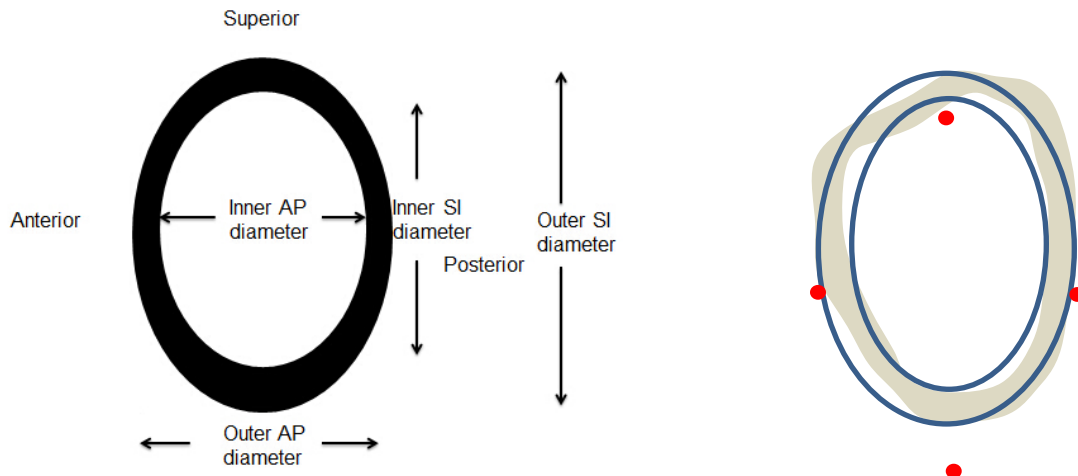
- 357 10. Bergmann G, Graichen F, Rohlmann A. Is staircase walking a risk for the fixation of hip
358 implants? J Biomech. 1995a; 28: 535-553.
- 359 11. Bergmann G, Kniggenndorf H, Graichen F, Rohlmann A. Influence of shoes and heel
360 strike on the loading of the hip joint. J Biomech. 1995b; 28: 817-827.
- 361 12. Bergmann G, Deuretzbacher G, Heller M, Graichen F, Rohlmann A, Strauss J, Duda G.
362 Hip contact forces and gait patterns from routine activities. J Biomech. 2001; 34: 859-
363 871.
- 364 13. Novak AC, Brouwer B. Sagittal and frontal lower limb joint moments during stair ascent
365 and descent in young and older adults. Gait & Posture. 2011; 33: 54-60.
- 366 14. Protopapadaki A, Drechsler IW, Cramp CM, Fiona J, Coutts J F, Scott MO. Hip, knee,
367 ankle kinematics and kinetics during stair ascent and descent in healthy young
368 individuals. Clin Biomech. 2007; 23: 203-210.
- 369 15. Duda GN, Heller M, Albinger J, Schulz O, Schneider E, Claes L. Influence of muscle
370 forces on femoral strain distribution. J Biomech. 1998; 31(9): 841-846.
- 371 16. Anderson DE, Madigan ML. Effects of age-related differences in femoral loading and
372 bone mineral density on strains in the proximal femur during controlled walking. J Appl
373 Biomech. 2013; 29: 505-516.
- 374 17. Winter DA, Sidwall HG, Hobson DA. Measurement and reduction of noise in kinematics
375 and locomotion. J Biomechanics. 1974; 7: 157-159.
- 376 18. Yu B, Gabriel D, Noble L, An KN. Estimate of the Optimum Cutoff Frequency for the
377 Butterworth Low-Pass Digital Filter. J Appl Biomech. 1999; 15(3): 318-329.
- 378 19. Vaughan C, Davis B, O'Connor J. Dynamics of human gait. 2nd ed. Cape Town, South
379 Africa: Kiboho Publishers; 1992.

- 380 20. Arnold EM, Ward SR, Lieber RL, Delp SL. A Model of the Lower Limb for Analysis of
381 Human Movement. *Ann Biomed Eng.* 2010; 38(2): 269–279.
- 382 21. Glitsch U, Baumann W. The three-dimensional determination of internal loads in the
383 lower extremity. *J Biomech.* 1997; 30: 1123–1131.
- 384 22. Beck TJ, Looker AC, Ruff CB, Sievanen H, Wahner HW. Structural trends in the aging
385 femoral neck and proximal shaft: analysis of the Third National Health and Nutrition
386 Examination Survey dual-energy X-ray absorptiometry data. *J Bone Miner Res.* 2000;
387 15: 2297-2304.
- 388 23. Bell KL, Loveridge N, Power J, Garrahan N, Stanton M, Lunt M, Meggitt BF, Reeve J.
389 Structure of femoral neck in hip fracture: cortical bone loss in the inferior-anterior to
390 superior-posterior Axis. *J Bone Miner Res.* 1999; 14(1): 111-119.
- 391 24. Derrick TR, Edward BW, Fellin RE, Seay JF. An integrative modeling approach for the
392 efficient estimation of cross sectional tibial stresses during locomotion. *J Biomech.* 2016;
393 49: 429-435.
- 394 25. Hall M, Stevermer CA, Gillette JC. Muscle activity amplitudes and co-contraction during
395 stair ambulation following anterior cruciate ligament reconstruction. *J Electromyogr*
396 *Kines.* 2015; 25: 298–304.
- 397 26. Delp SL, Maloney W. Effects of hip center location on the moment-generating capacity
398 of the muscles. *J Biomech.* 1993; 26 485-499.

399

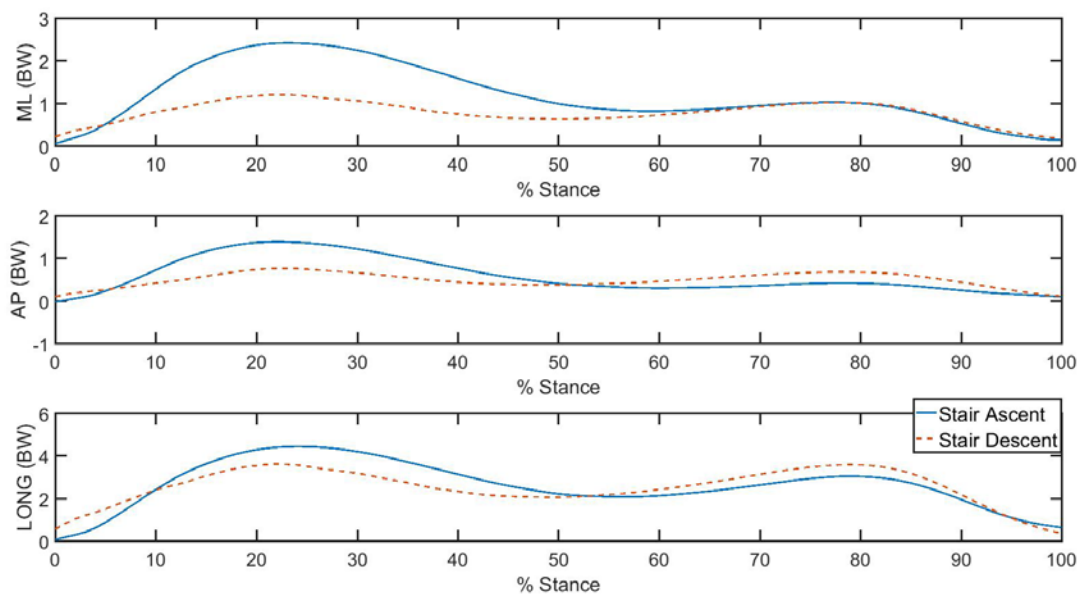
400

Figures



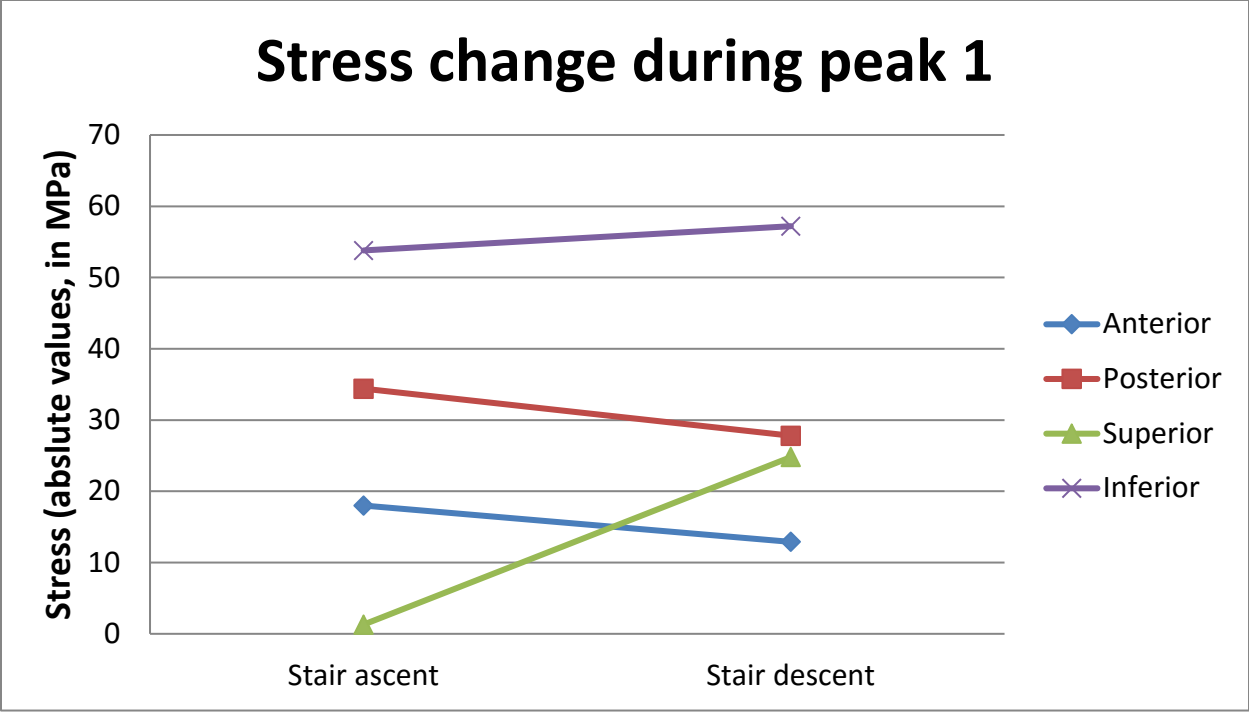
401

402 **Figure 1.** Elliptical bone model superimposed on a cross-sectional CT scan of the femoral neck.



403

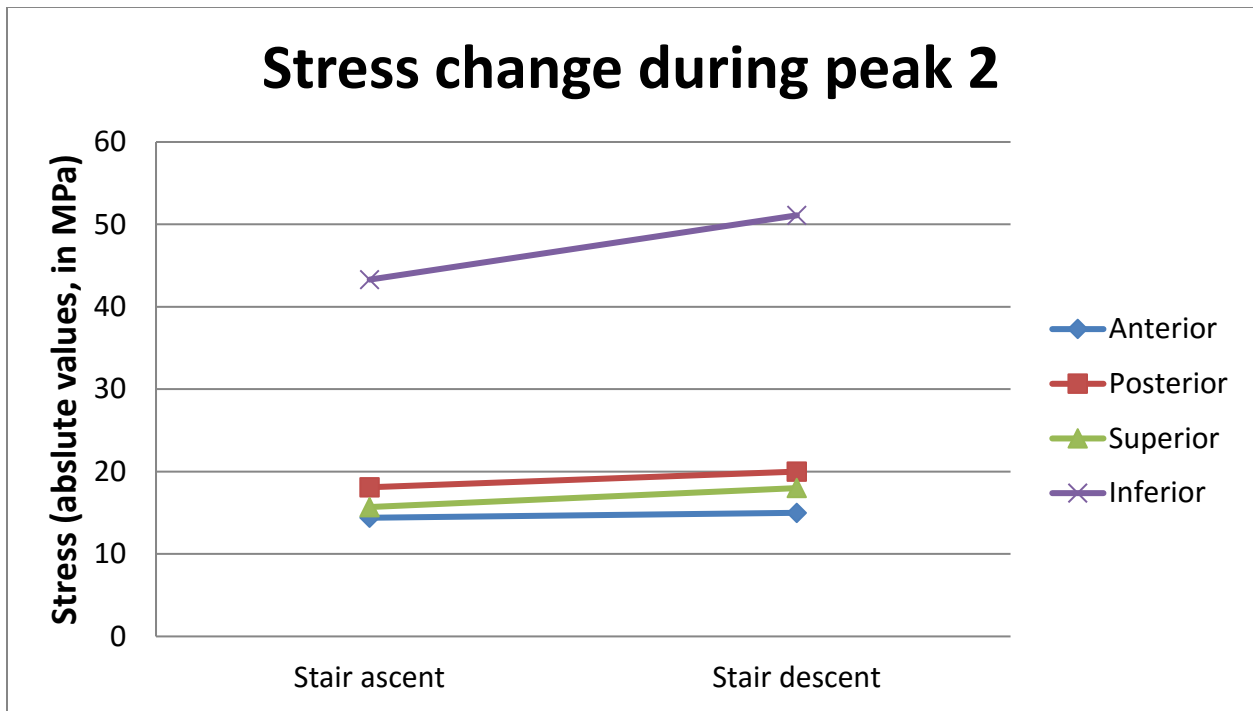
404 **Figure 2.** Ensemble average of contact forces at 3 planes of the hip joint. ML stands for Medial-Lateral direction,
405 AP stands for Anterior-Posterior direction, LONG stands for longitudinal direction. Positive values indicate
406 lateral, posterior, and downward directions.



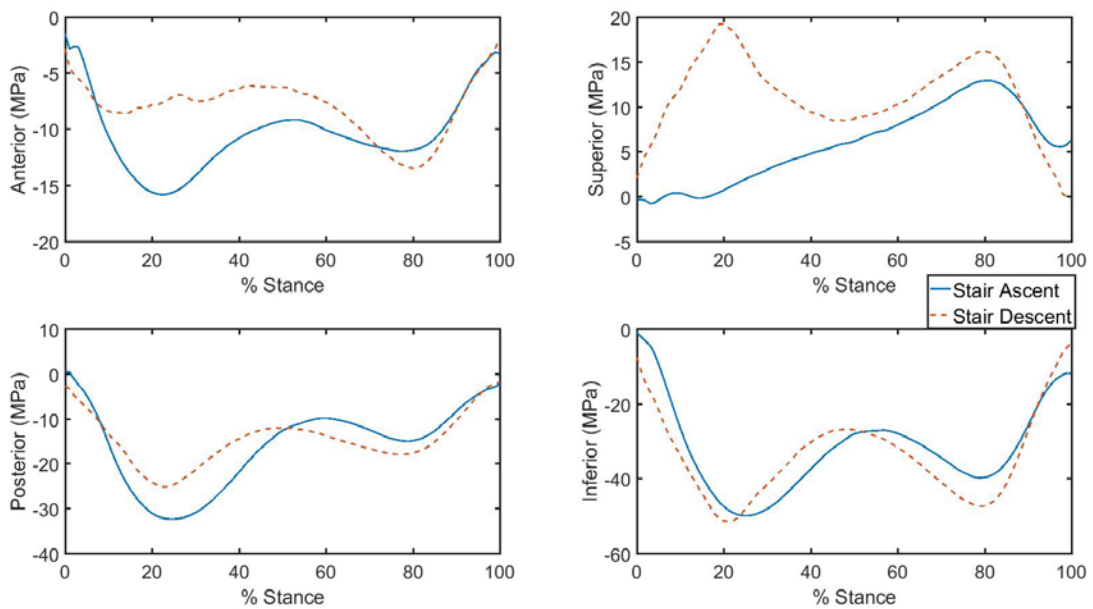
407

408 **Figure 3.** Change of stress between stair ascent and descent during stress peak 1 for the anterior, posterior,
409 superior and inferior regions of the femoral neck.

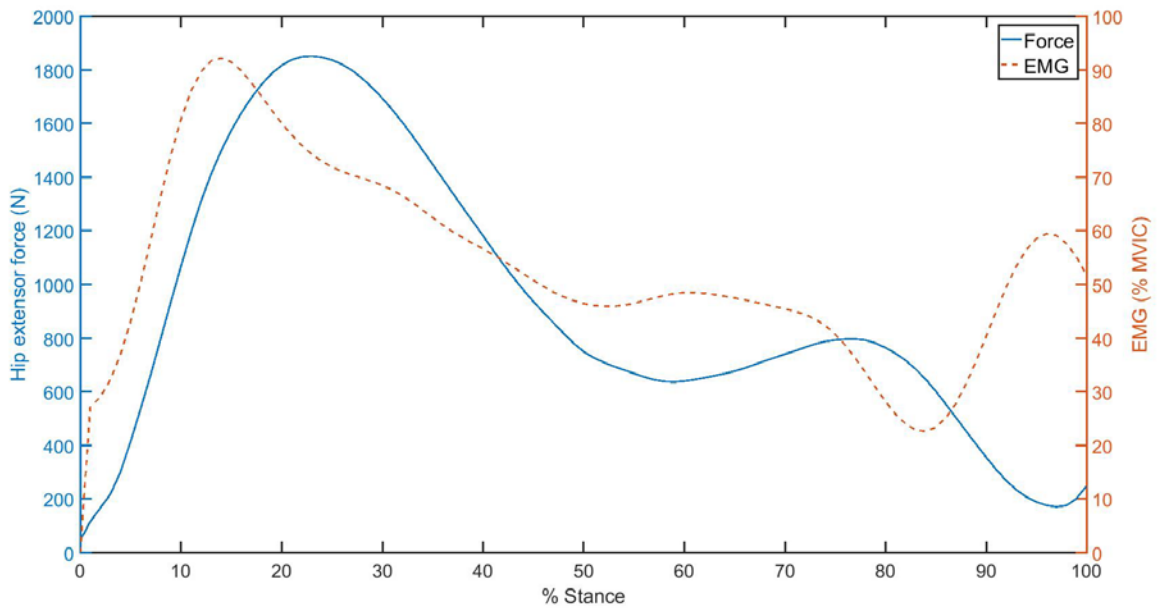
410



411
 412 **Figure 4.** Change of stress between stair ascent and descent during stress peak 2 for the anterior, posterior,
 413 superior and inferior regions of the femoral neck.



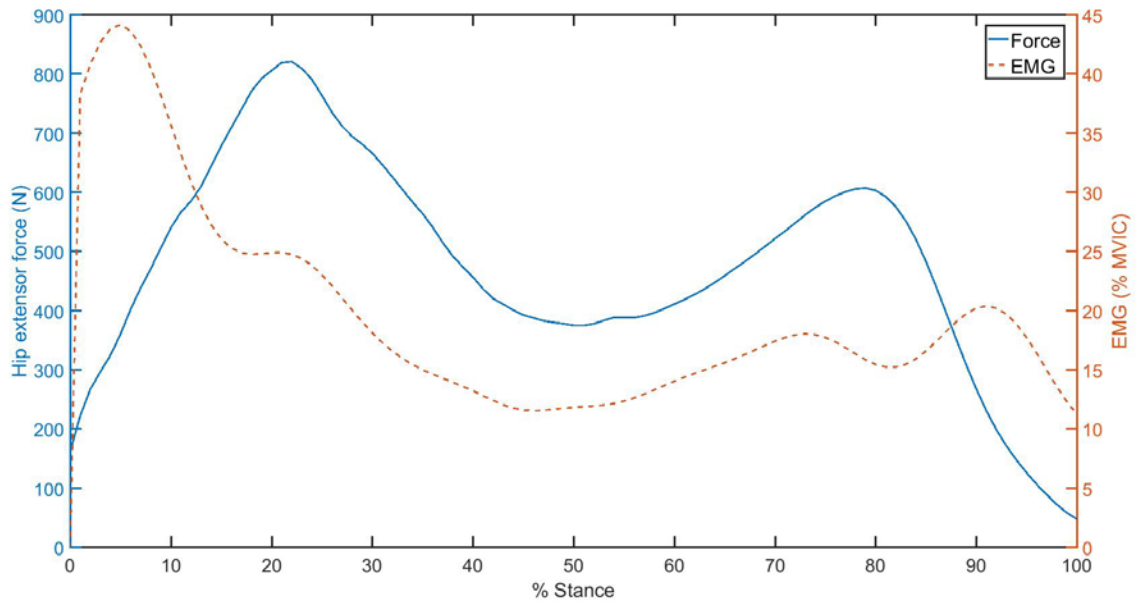
414
 415 **Figure 5.** Ensemble average of stresses at superior and inferior sites of femoral neck, positive values indicate
 416 tension, negative indicate compression.



417

418 **Figure 6.** Average of estimated hip extensor muscle forces (in Newtons) and EMG activities (in % MVIC) [19]

419 during stair ascent.



420

421 **Figure 7.** Average of estimated hip extensor muscle forces (in Newtons) and EMG activities (in % MVIC) [19]

422 during stair descent.

423

Tables

424 **Table 1.** Means (SD) of muscle caused and reaction force caused stresses (MPa) on 4 sites on the femoral neck during stair ascent and descent for peak 1. Bolded

425 values and corresponding p-values indicate significant differences between stair ascent and descent stresses.

Stress Site	Peak 1 Stress Components													
	Stair Ascent Stress (MPa)							Stair Descent Stress (MPa)						
	Muscle			Reaction				Muscle			Reaction			
	Force Source	Moment Source	Total Muscle	Force Source	Moment Source	Total Reaction	Total	Force Source	Moment Source	Total Muscle	Force Source	Moment Source	Total Reaction	Total
Superior	-20.6 (4.5)	-42.6 (15.7)	-63.1 (18.5)	-2.9 (0.6)	67.3 (18.5)	64.4 (17.1)	1.3¹ (7.0)	-10.7 (3.2)	-31.9 (16.0)	-42.7 (19.0)	-3.8 (1.0)	71.3 (24.0)	67.5 (24.7)	24.8¹ (9.7)
Inferior	-21.7 (4.9)	54.5 (20.6)	32.8 (17.2)	-3.4 (0.6)	-83.2 (22.9)	-86.6 (23.4)	-53.8 (12.2)	-13.0 (3.0)	36.4 (18.1)	23.5 (16.4)	-4.1 (0.9)	-76.6 (25.8)	-80.6 (26.2)	-57.2 (15.1)
Anterior	-20.0 (6.2)	28.0 (12.2)	8.0 (9.0)	-3.0 (1.1)	-23.0 (12.1)	-26.0 (12.7)	-18.0¹ (7.9)	-12.3 (2.6)	-2.3 (12.5)	-14.6 (11.0)	-3.1 (1.1)	4.9 (13.9)	1.8 (14.4)	-12.9¹ (5.4)
Posterior	-21.9 (4.9)	-26.8 (13.4)	-48.7 (17.3)	-3.4 (0.6)	17.7 (16.0)	14.3 (15.8)	-34.4¹ (10.9)	-13.4 (3.0)	7.1 (12.4)	-6.3 (13.2)	-4.0 (0.8)	-17.6 (15.6)	-21.6 (15.8)	-27.8¹ (10.1)

426 1. p < 0.001

427

428 **Table 2.** Means (SD) of muscle caused and reaction force caused stresses (MPa) on 4 sites on the femoral neck during stair ascent and descent for peak 2. Bolded
 429 values and corresponding p-values indicate significant differences between stair ascent and descent stresses.

Stress Site	Peak 2 Stress Components													
	Stair Ascent Stress (MPa)							Stair Descent Stress (MPa)						
	Muscle			Reaction				Muscle			Reaction			
	Force Source	Moment Source	Total Muscle	Force Source	Moment Source	Total Reaction	Total	Force Source	Moment Source	Total Muscle	Force Source	Moment Source	Total Reaction	Total
Superior	-9.9 (2.1)	-33.9 (16.4)	-43.8 (17.8)	-3.0 (0.8)	62.6 (20.0)	59.5 (19.3)	15.7¹ (6.1)	-13.2 (3.4)	-15.2 (10.5)	-28.4 (12.1)	-2.7 (0.6)	49.2 (18.6)	46.5 (18.2)	18.0¹ (8.4)
Inferior	-10.9 (2.4)	40.1 (15.8)	29.2 (14.3)	-3.4 (0.6)	-69.6 (18.6)	-73.0 (19.1)	-43.8² (9.7)	-13.9 (3.4)	16.1 (11.3)	2.3 (10.3)	-2.8 (0.6)	-50.6 (19.3)	-53.3 (19.9)	-51.1² (14.3)
Anterior	-9.2 (2.8)	5.0 (9.5)	-4.2 (8.7)	-2.8 (0.8)	-7.4 (11.1)	-10.2 (11.6)	-14.4 (7.7)	-13.2 (2.8)	-30.2 (11.8)	-43.6 (13.2)	-2.6 (0.6)	31.0 (11.6)	28.5 (11.4)	-15.0 (5.3)
Posterior	-10.6 (2.3)	-6.3 (9.7)	-16.9 (10.3)	-3.0 (0.7)	1.8 (11.3)	-1.2 (11.3)	-18.1 (8.6)	-13.2 (3.3)	30.0 (12.5)	16.7 (11.4)	-2.7 (0.8)	-34.0 (14.5)	-36.7 (14.8)	-20.0 (7.6)

430 1. $p < 0.029$

431 2. $p < 0.005$

432